0026-895X/97/050807-08$3.00/0

MOLECULAR PHARMACOLOGY, **52:**807–814 (1997).

Ligand Binding Pocket of the Human Somatostatin Receptor 5: Mutational Analysis of the Extracellular Domains

MICHAEL T. GREENWOOD, NEDIM HUKOVIC, UJENDRA KUMAR, ROSEMARIE PANETTA, SIV A. HJORTH, COIMBATORE B. SRIKANT, and YOGESH C. PATEL

Fraser Laboratories, Departments of Medicine and Neurology and Neurosurgery, McGill University, Royal Victoria Hospital, and the Montreal Neurological Institute, Montreal, Quebec H3A 1A1, Canada (M.T.G., N.H., U.K., R.P., C.B.S., Y.C.P.), and Laboratory for Molecular Pharmacology, The Laboratory Center, Rigshospitalet, Copenhagen, DK-2100, Denmark (S.A.H.)

Received November 15, 1996; Accepted July 30, 1997

SUMMARY

The ligand binding domain of G protein-coupled receptors for peptide ligands consists of a pocket formed by extracellular and transmembrane domain (TM) residues. In the case of somatostatin (SRIF), however, previous studies have suggested that the binding cavity of the octapeptide analog SMS201–995 (SMS) is lined by residues in TMs III–VII. The additional involvement of the extracellular domains for binding SMS or the natural SRIF ligands (SRIF-14, SRIF-28) has not been clarified. Using a cassette construct cDNA for the human somatostatin 5 receptor (sst_5R), we systematically examined the role of exofacial structures in ligand binding by creating a series of mutants in which the extracellular portions have been altered by conservative segment exchange (CSE) mutagenesis for the extracellular loops (ECLs) and by deletion (for the NH_2-terminal segment) or truncation analysis (ECL3). CHO-K1 cells were stably transfected with wild type or mutant human sst_5R constructs, and agonist binding was assessed using membrane binding assays with ^{125}I-LTT SRIF-28 ligand. Deletion of the NH_2 terminus or CSE mutagenesis of ECL1 and ECL3 produced minor 2–8-fold decreases in affinity for SRIF-14, SRIF-28, and SMS ligands. Truncation of ECL3 to mimic the size of this loop in sst_1R and sst_4R (the two subtypes that do not bind SMS) did not interfere with the binding of SMS, SRIF-14, or SRIF-28. In contrast, both ECL2 mutants failed to bind ^{125}I-LTT SRIF-28. Immunocytochemical analysis of nonpermeabilized cells with a human sst_5R antibody revealed that the mutant receptors were targeted to the plasma membrane. Labeled SMS (^{125}I-Tyr3 SMS) also failed to bind to the mutant ECL2 receptors. These results suggest a potential contribution of ECL2 (in addition to the previously identified residues in TMs III–VII) to the SRIF ligand binding pocket.

GPCRs are thought to be integral membrane proteins that span the lipid bilayer seven times and give rise to an extracellular amino-terminal domain, three ECLs, three intracellular loops, and an intracellular carboxyl-terminal domain (1). Such a model is based on a limited amount of biochemical and biophysical data including a low resolution map of rhodopsin, although in the absence of high resolution crystallography, the exact structure of these receptors remains speculative (2). The structure of an apparently unrelated seven-TM protein, bacteriorhodopsin, has been determined at high resolution, and structural models of GPCRs have been created using bacteriorhodopsin coordinates (3). In the absence of crystallographic data, most investigators have therefore resorted to indirect methods such as site-directed mutagenesis and receptor chimeras to elucidate the structural and functional domains of GPCRs (4–9). Based on such studies, it has been suggested that the ligand binding site of GPCRs consists of a number of noncontiguous amino acid residues that form a binding pocket within the folded receptor (6, 7). In the case of rhodopsin and bioamine receptors, such a binding pocket lies deep within the plasma membrane and is made up exclusively of residues within the TMs. In contrast, large protein ligands such as glycoprotein hormones interact principally with the amino-terminal segment. For peptide receptors, however, the ligand binding pocket typically involves residues in the ECLs or both ECLs and TMs (7–9).

The neuropeptide SRIF interacts with a family of GPCRs with five current members termed sst receptor subtypes 1–5 (10). The receptors share a high degree of sequence identity

This work was supported by Grants MT 10411 and MT 12603 from the Canadian Medical Research Council and Grant NS32160 from the National Institutes of Health. M.T.G. and N.H. contributed equally. Both are Fellows of the Fonds de la Recherche en Santé du Quebec. Y.C.P. is a Distinguished Scientist of the Canadian Medical Research Council.

ABBREVIATIONS: GPCR, G protein-coupled receptor; ECL, extracellular loop; TM, transmembrane domain; CHO, Chinese hamster ovary; SRIF, somatostatin; SMS, SMS201–995; CSE, conservative segment exchange; sstR, somatostatin receptor; $hsst_5R$, human somatostatin 5 receptor; sst_xR, somatostatin receptor, where *x* is the number of the receptor; PCR, polymerase chain reaction; PBS, phosphate-buffered saline; BSA, bovine serum albumin; AT, angiotensin; HEPES, 4-(2-hydroxyethyl)-1-piperazineethanesulfonic acid.

in the TMs (55–70%) and diverge the most within the extracellular segments. Four of the five sst receptors (subtypes 1–4) display approximately equal affinity for both naturally occurring SRIF ligands, SRIF-14 and SRIF-28 (10–13). The sst_5R displays the same affinity for SRIF-14 as the other sst receptors but has a 2–30-fold higher affinity for SRIF-28 (10, 11). Conformationally restricted analogs like the octapeptide SMS (octreotide) or hexapeptide MK678 (seglitide) bind to only three of the sst receptor subtypes: 2, 3, and 5. By exploiting the differential ability of SMS to bind to sst_2R but not to sst_1R, Kaupmann *et al.* (14) systematically mutated the sst_1R to resemble sst_2R. Their findings suggest that the binding pocket for SMS involves residues located exclusively within TMs III–VII. Of the eight residues postulated to form the binding pocket, experimental evidence, however, exists for the involvement of only three of these: an aspartic acid in TM III, which is predicted to interact with lysine in the Phe-Trp-Lys-Thr core of both ligands, and asparagine and phenylalanine located at the outer end of TMs VI and VII, respectively (present in sst_2R but not sst_1R), necessary for binding of both ligands (14–16). A potential role of nonconserved residues, including most of the ECLs, has not been evaluated. Furthermore, the question of whether sst receptor subtypes 3–5 share a similar ligand binding pocket with sst_1R and sst_2R remains to be determined. Because SRIF-14 binds with roughly equal affinity to all five sst receptors, it is probable that the binding pocket for this ligand is identical in the five receptors. On the other hand, the ligand binding pocket of other GPCRs that recognize the same ligand has been shown to consist of some nonconserved residues, suggesting that the ligand binding pocket of one GPCR cannot always be used to predict the location of the pocket for the same ligand on a closely related member of the same subfamily (17–19). In all cases so far examined, at least a portion of the extracellular region of a GPCR is required to interact with peptide ligands like SRIF (4, 8, 9, 20). Accordingly, in the current study, we systematically examined the role of exofacial structures in ligand binding using as a model $hsst_5R$. With a series of $hsst_5R$ mutants in which the entire NH_2-terminal segment has been deleted or the ECLs have been altered by CSE mutagenesis (20), we report that a major fraction of the extracellular domain of $hsst_5R$ does not play a role in ligand binding but that mutations in the second ECL abolish high affinity ligand binding.

Experimental Procedures

Materials. SRIF-14 was from Ayerst Laboratories (Montreal, Canada). SRIF-28 and Leu^8-D-Trp^{22},Tyr^{25}-SRIF-28 (LTT SRIF-28) was from Bachem (Marina Del Ray, CA). SMS and Tyr^3-SMS were from Sandoz (Basel, Switzerland). MK678 was from Merck Frosst Laboratories (Montreal, Canada). Mouse monoclonal antibody to vimentin was purchased from Sigma Chemical (St. Louis, MO) and obtained as a gift from Dr. D. Laird (McGill University, Montreal Quebec, Canada).

Construction of $hsst_5r$ cassette cDNA. A cassette construct cDNA was created consisting of the entire coding sequence of $hsst_5r$ in which silent mutations had been introduced to generate unique restriction sites to facilitate the manipulation of the sequence as discrete restriction fragments (Fig. 1) (20). Mutations were introduced into a specific $hsst_5R$ restriction fragment by PCR and subsequently used to replace the corresponding wild-type fragment in the cassette construct. The choice of restriction sites was dictated by their absence in the expression vector (see below) and by the fact that the creation of the site by mutagenesis would not alter the amino acid sequence of the receptor. Five fragments encompassing the entire $hsst_5R$ coding sequence were generated by PCR as follows: a *Hin*dIII/*Kpn*I fragment containing the translational initiation codon as well as a Kozak consensus sequence (21) up to nucleotide 126, a *Kpn*I/*Eco*RV fragment containing nucleotides 126–410, an *Eco*RV/*Bst*XI fragment containing nucleotides 410–540, a *Bst*XI/*Mlu*I fragment containing nucleotides 540–739, and an *Mlu*I/*Eco*RI fragment containing nucleotides 739-1092, including the translational termination codon. All five fragments were ligated by PCR (20); a restriction map of the resultant construct is shown in Fig. 1. Sequence analysis was used to confirm the structure of the cassette construct (University Core DNA Service, University of Calgary, Calgary, Alberta, Canada). The cDNA was then cloned into the *Hin*dIII/*Eco*RI sites of pTEJ8, a mammalian expression vector that uses the human ubiquitin promoter to drive expression (22).

Generation of $hsst_5R$ mutants. To characterize the role of the exofacial structures of $hsst_5R$ in ligand binding, a series of mutants of the NH_2-terminal segment and ECL1–3 were constructed as follows.

NH_2-terminal deletion mutant. An NH_2-terminal $hsst_5R$ mutant (Δ5NT) was constructed in which the NH_2-terminal 36 residues were removed by deletion of a portion of the cassette construct. Of the predicted 39 NH_2-terminal residues, only three were retained (Fig. 2).

ECL1–3 conservative segment exchange mutants. The technique of CSE mutagenesis was used to systematically evaluate the role of the three ECLs of $hsst_5R$ in ligand binding (20). In CSE mutagenesis, large stretches of residues are replaced by chemically similar residues, with the exception of residues with no chemically similar counterparts (proline, glycine, and cysteine), which are not altered (Fig. 2). The ECL1 of $hsst_5R$ consists of 13 residues that include a conserved cysteine residue found in the ECL1 of most GPCRs as well as the highly conserved WPXG motif (23). Because these residues may play major structural roles in the receptor (20), they were not altered in the CSE mutant for ECL1 (mut1) (Fig. 2B). The ECL2 region with 19 residues was divided into two portions, and two distinct mutants were constructed. Six of the 9 NH_2-terminal residues were conservatively altered to create mutant mut2N, whereas 7 of the 10 COOH-terminal residues were mutated to create mut2C (Fig. 2B). In the case of ECL3, 7 of the 9 residues were conservatively mutated to create mutant mut3 (Fig. 2). CSE mutagenesis has proved to be valuable in identifying key regions involved in the ligand binding domain of receptors such as the AT_1 receptor (20). Its advantage lies in the ability to mutate long stretches of amino acids without grossly altering receptor structure.

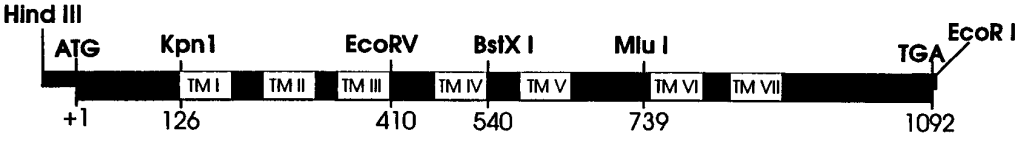

Fig. 1. Structure of the $hsst_5R$ cassette construct. The locations of the new restriction sites introduced via silent mutations are shown with respect to TMI–VII. A Kozak consensus sequence (GCCGCCACC) was also introduced directly 5′ to the translational initiation codon (ATG). *Bottom*, the structure is numbered in nucleotides (base pairs). The entire $hsst_5R$ cassette construct was subcloned into the unique *Hin*dIII/*Eco*RI sites of the polylinker region of the mammalian expression vector pTEJ8.

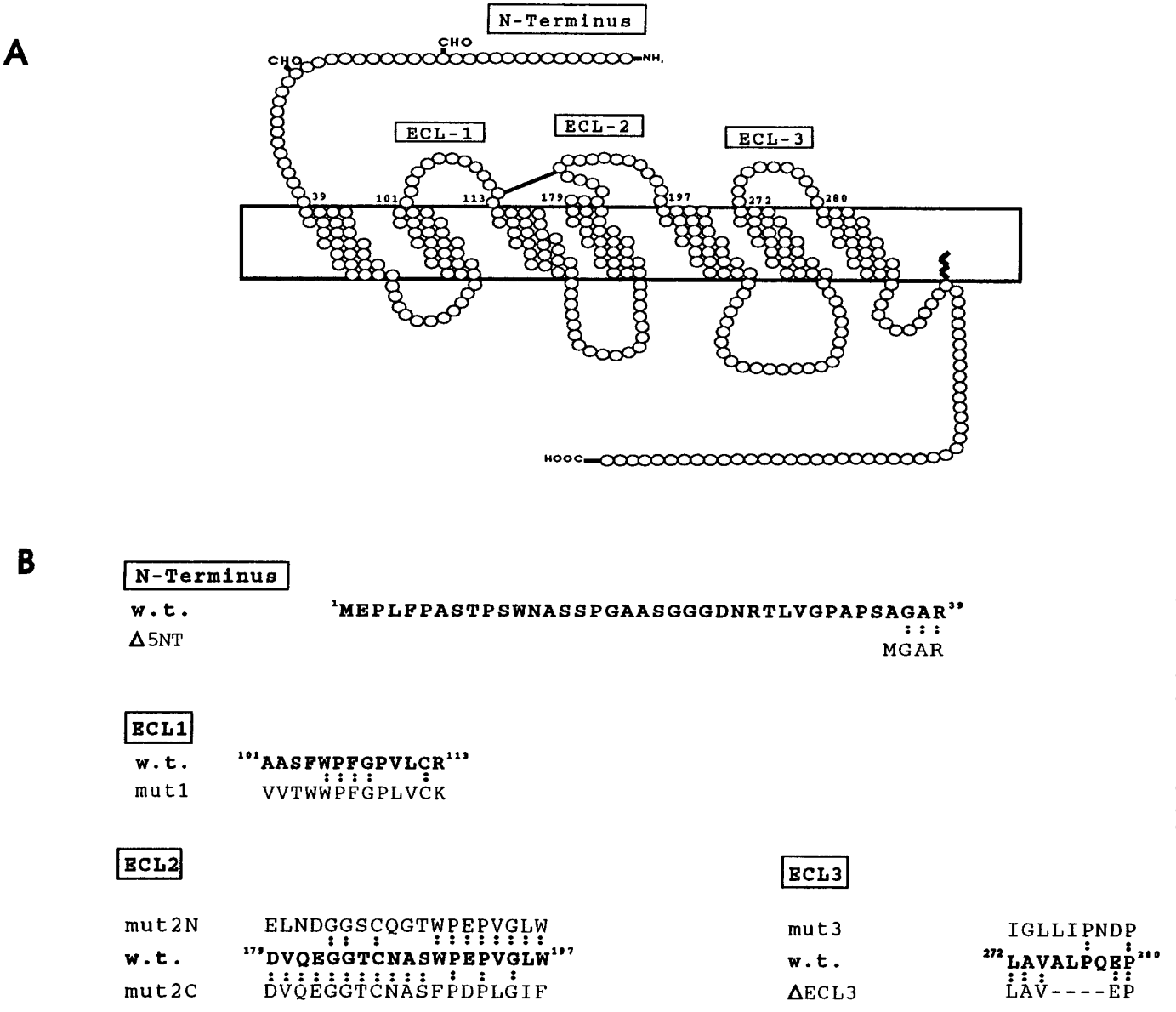

Fig. 2. Putative membrane topography of hsst$_5$R and comparison of the sequences of the hsst$_5$R mutants with their wild-type counterparts. A, Location and borders of extracellular regions. *NH$_2$*, amino terminus; *HOOC*, carboxyl terminus; *CHO*, putative glycosylation site; also depicted is the potential palmitoylation site in the intracellular carboxyl-tail, which serves as a membrane anchor. B, Alignment of the ECL, NH$_2$-terminal deletion, and ECL3 deletion mutants with their wild-type (*w.t.*) counterparts reveals residues that were conserved (:) as well as the conservative exchanges. *Bold*, wild-type sequences are numbered according to their location in the receptor sequence (11). Thirty-five residues of the amino terminus of hsst$_5$R were removed to create the mutant Δ5nt del. An A36M mutation was introduced to create the new translational initiation codon of the mutant; therefore, only 3 of 39 amino-terminal hsst$_5$R residues remain in the mutant.

Limitations of the technique include the inability to substitute residues proline, glycine, and cysteine or the WPXF motif in ECL1 as well as the generation of false-negative results because the chemical nature rather than the exact residue may be important in determining its ligand binding affinity.

ECL3 deletion mutant. An hsst$_5$R mutant (ΔECL3) was constructed in which four amino acid residues were removed from ECL3 to mimic the size of the loop in hsst$_1$R and hsst$_4$R (Fig. 2).

Next, hsst$_5$R subfragments containing desired mutations were constructed using the PCR overlap extension technique (25, 26). The *Hin*dIII/*Eco*RV fragment of the cassette construct was used to create mut1, the *Eco*RV/*Mlu*I fragment was used to create the ECL2 mutants, and the *Mlu*I/*Eco*RI fragment was used to create the ECL3 and ECL3 deletion mutants. To construct the NH$_2$-terminal deletion mutant Δ5NT, a 5′-end *Hin*dIII/*Eco*RV fragment was generated by PCR using an oligonucleotide with a translational initiation codon located at nucleotide 106 of the hsst$_5$R coding sequence, thereby producing a 35-amino acid truncation of the amino terminus. A Kozak consensus sequence was included 5′ to the new translational initiation codon. Mutated DNA fragments were used to replace the corresponding wild-type restriction fragments in the cassette construct in the expression vector pTEJ8. Sequence analysis was used to confirm the structure of the mutated DNAs. The wild-type and mutant receptor cDNAs were then used to stably transfect CHO-K1 cells to G418 resistance (11), and nonclonally selected cells were prepared for study.

Binding assays. CHO-K1 cells expressing wild-type and mutant hsst$_5$R constructs were cultured in D-75 flasks to 70% confluency in Ham's F-12 medium containing 10% fetal calf serum and 400 μg/ml G418. The cells were washed and harvested by centrifugation, and

membranes were prepared by homogenization. Binding studies were carried out for 30 min at 30° with 20–40 μg of membrane protein and ^{125}I-LTT SRIF-28 in 50 mM HEPES-KOH buffer, pH 7.5, containing 5 mM Mg^{2+}, 0.02% BSA, 200 kallikrein inhibitor units/ml aprotinin, 0.02 μg/ml phenylmethylsulfonyl fluoride, and 0.02 μg/ml bacitracin (11, 12, 27). Incubations were terminated by the addition of 1 ml of ice-cold HEPES-KOH containing 0.2% BSA, rapid centrifugation, and washing. Radioactivity associated with membrane pellets was quantified in an LKB γ-counter (LKB-Wallac, Turku, Finland) with a counting efficiency of 69% and background of <50 cpm Specific binding is defined as the difference between counts bound in the absence and presence of 100 nM SRIF-28. Saturation binding experiments were performed with membranes using increasing concentrations of ^{125}I-LTT SRIF-28 (2–2000 pM) under equilibrium binding conditions as described previously (11, 12, 27). Competition analyses were carried out through incubation of membranes with ^{125}I-LTT SRIF-28 (~60 pM) and increasing concentrations of SRIF-14, SRIF-28, and SMS. Binding data were analyzed with INPLOT 4.03 (GraphPAD Software, San Diego, CA). As reported previously, the affinity of LTT SRIF-28 for sst_5 is 3-fold greater than that of SRIF-28 (12).

Generation of $hsst_5$R-specific antibodies. Peptide [^{3}H]GLFPASTPSKK (G5nt) containing the extracellular amino-terminal segments 4–11 of the deduced sequence of $hsst_5$R with an [^{3}H]Gly addition at the NH_2 terminus (to monitor coupling to protein) and a Lys-Lys addition at the COOH terminus was synthesized by solid phase and covalently conjugated to BSA with glutaraldehyde. Peptide YLFPASTPSKK (Y5nt) was synthesized for radioiodination. The G5nt-BSA conjugate was emulsified with complete Freund's adjuvant (2 mg/ml) and injected subcutaneously into 3-kg New Zealand White rabbits. Booster injections were administered every 4 weeks. The rabbits were bled from the central ear artery before immunization (preimmune serum) and 2 weeks after each boost. Antibody production was monitored by immunoprecipitation of ^{125}I-Y5nt. Serum harvested at 7 months from one of the immunized rabbits was selected for immunocytochemistry.

Immunofluorescent labeling and confocal microscopy for sstR expression. Cell surface expression of mutant sst receptor protein was determined by immunocytochemistry of live unfixed cells. CHO-K1 cells stably transfected with wild-type $hsst_5$R or $hsst_5$r mutants were cultured to ~70% confluency, washed twice in PBS, and incubated with $hsst_5$r primary antibody (1:200) in serum-free culture medium for 8–10 hr at 4° (28). Cultures were then rinsed twice in PBS and fixed with either methanol acetone (4:1) or freshly prepared paraformaldehyde (4% in 0.1% PBS) for 20 min. After three washes in 50 mM Tris·HCl and 1.5% NaCl, pH 7.4, cells were incubated for 90 min at 20° with rhodamine-conjugated goat anti-rabbit secondary antibody (1:100). Cells were finally washed thrice in 50 mM Tris·HCl and 1.5% NaCl, pH 7.4, and mounted with Immunofluor for confocal microscopy. Preimmune serum, antigen-absorbed antibody, and nontransfected CHO-K1 cells were used as controls. To monitor the integrity of the plasma membrane, unfixed cells were immunostained with an antibody to the intermediate filament protein vimentin (1:200), followed by incubation with goat anti-mouse fluorescein isothiocyanate-conjugated IgG (1:100). In addition, both sstR and vimentin immunoreactivities were localized in CHO-K1 cells permeabilized with 0.2% Triton X-100 for 5 min at 20° and processed under identical conditions. All fluorescent images were visualized on a Zeiss LSM 410 inverted confocal microscope equipped with an argon/krypton laser. Rhodamine signal was imaged on a photomultiplier after passage through FT510, FT560, and FT590 filter sets. Images were obtained as single optical sections taken through the middle of the cells and averaged over 32 scans/frame. All images were collected and handled identically. They were archived on a Bernoulli multidisc and printed on a Kodak XL58300 high resolution (300 dpi) color printer.

Results

Pharmacological characterization of wild-type and mutant forms of $hsst_5$R. Total and nonspecific binding of ^{125}I-LTT SRIF-28 to membranes prepared from stable CHO-K1 cells transfected with cDNAs for the $hsst_5$R cassette construct and the $hsst_5$R mutants is shown in Fig. 3. Except for the two ECL2 mutants (mut2N, mut2C) wild-type $hsst_5$R and all other mutants displayed specific binding of ^{125}I-LTT SRIF-28 ligand. Comparable binding was obtained with a second ligand, ^{125}I-Tyr3 SMS, which also failed to bind to the ECL2 mutants. Saturation analysis of the $hsst_5$R revealed high levels of expression of membrane receptors with a B_{max} value of 119 ± 24 fmol/mg of protein and a K_d value of 0.335 ± 0.075 nM (Table 1). These values are consistent with our previous characterization of $hsst_5$R (9). The receptor expressed from the $hsst_5$R cassette construct bound SRIF-28 ≥ SRIF-14 > SMS (Table 2).

NH_2-terminal deletion mutant. Saturation binding analysis with membranes prepared from CHO-K1 cells expressing the Δ5NT mutant revealed high levels of expression of the mutant receptor (290 fmol/mg of protein), which exhibited high affinity binding of ^{125}I-LTT SRIF-28 ligand comparable to that of the wild-type receptor (Table 1). The binding affinities of the mutant receptor for SRIF-14, SRIF-28, and SMS obtained by displacement analysis revealed only a minor (<2-fold) change compared with wild-type (Fig. 4 and Table 2), indicating that the amino-terminal domain of $hsst_5$R is not critical for high affinity binding of these ligands (29).

ECL1. Saturation analysis revealed that the mutant receptor mut1 retained a high level of membrane expression (B_{max} = 144 fmol/mg of protein) as well as high affinity for ^{125}I-LTT SRIF-28 (Table 1). The affinity of mut1 was further assessed by competitive binding analysis and showed a slight (<-2.5-fold) decrease in affinity for SRIF-14, SRIF-28, and SMS, indicating that ECL1 similarly is not critical for high affinity agonist binding.

ECL3. Proper expression and targeting of the ECL3 CSE mutant mut3 were similarly suggested by saturation binding analysis that showed a B_{max} value of 106 fmol/mg of protein

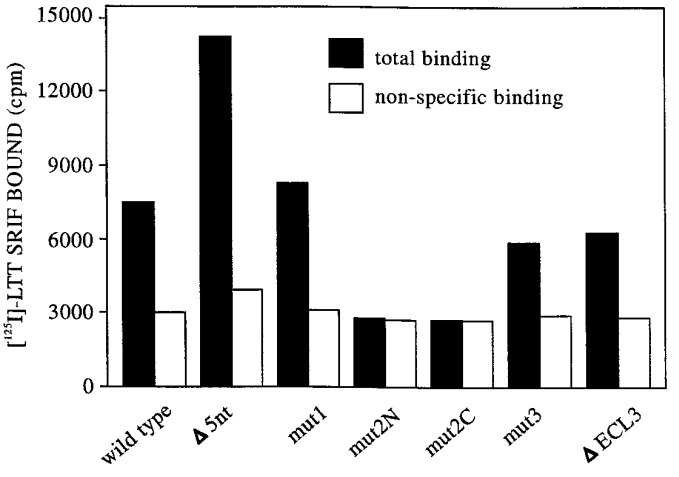

Fig. 3. Binding of ^{125}I-LTT SRIF-28 to membranes (40 μg of total protein) in the absence (total binding) or presence (nonspecific binding) of 100 nm SRIF-28 in wild-type and mutant sst_5R-expressing cells. Typical data are representative of duplicate measurements. See text for experimental details.

TABLE 1

Saturation analysis of hsst$_5$R and hsst$_5$R mutants

Experiments were performed under equilibrium binding conditions with increasing amounts of ^{125}I LTT SRIF-28 (2–2000 pM). The values represent the mean of two separate experiments performed in triplicate and showed <10% variation.

Mutant	B_{max}	K_d
	fmol/mg	*nM*
Wild-type	119	0.335
Δ5nt	290	2.6
mut1	144	1.47
mut2N	N.D.	N.D.
mut2C	N.D.	N.D.
mut3	106	1.025
ΔECL3	187	1.006

N.D., no specific binding.

TABLE 2

Comparison of the potencies of SST agonists for binding to hsst$_5$R and hsst$_5$R mutants

K_i values represent the inhibitory concentrations of the mutants required for half-maximal inhibition of ^{125}I LTT SRIF-28 binding. Values are mean ± standard error from three determinations.

Mutant	K_i		
	SRIF-14	SRIF-28	SMS
		nM	
Wild-type	0.9 ± 0.05	0.39 ± 0.07	5.0 ± 0.13
Δ5nt	0.8 ± 0.01	0.34 ± 0.02	8.8 ± 0.8
mut1	2.3 ± 0.2	0.99 ± 0.12	5.6 ± 0.37
mut2N	N.D.	N.D.	N.D.
mut2C	N.D.	N.D.	N.D.
mut3	3.6 ± 0.7	5.1 ± 0.13	21.0 ± 1.2
ΔECL3	12.0 ± 0.38	2.8 ± 0.08	15.0 ± 1.8

N.D., nondetectable binding.

and a 3-fold lower binding affinity (K_d) than the wild-type receptor (Table 1). Competitive binding analysis revealed that the affinity of mut3 for SRIF-14 and SMS decreased 4-fold, whereas the affinity for SRIF-28 decreased 8-fold (Fig. 4 and Table 2). This suggests that ECL3 also is not critically important for high affinity ligand binding. In addition to a role of specific amino acid residues, the size of the ECLs could be important in the formation of the binding pocket. For example, the subtypes hsst$_1$R and hsst$_4$R, which fail to bind conformationally restricted SRIF analogs, display noticeably shorter ECL3 segments, prompting speculation that a smaller ECL3 could sterically hinder ligand access to the proposed binding pocket in TMs 6 and 7 (24). To test this hypothesis, we constructed the ECL3 mutant. This mutant (ΔECL3) was readily expressed at the cell membrane, where it displayed a binding affinity similar to that of the wild-type receptor (Table 1). This mutant displayed a 12-fold decrease in affinity for SRIF-14 and SRIF-28 and an 8-fold decrease for SMS (Table 2 and Fig. 4). These changes are relatively small and indicate that the size of ECL3 cannot account for the reported >1000-fold lower affinity for short SRIF analogs such as SMS displayed by the two sstR subtypes (hsst$_1$R and hsst$_4$R) that feature relatively short ECL3 (23).

ECL2. No specific ^{125}I-LTT SRIF-28 binding could be detected in CHO-K1 cells stably transfected with mut2N and mut2C (Fig. 3 and Table 1). Because it is possible that such dramatic loss of binding is due to improper targeting of the mutant receptors to the plasma membrane, expression of receptor protein was analyzed immunocytochemically in live, unfixed cells. With the NH_2-terminally directed anti-peptide hsst$_5$R primary antibody, CHO-K1 cells expressing wild-type hsst$_5$R showed rhodamine immunofluorescence localized to the cell surface (Fig. 5A). The two ECL2 mutants also exhibited surface immunofluorescence with this antibody, indicating that the mutant receptors are properly localized to the plasma membrane (Fig. 5, B and C). Permeabilization of CHO-K1 cells expressing wild-type or the two mutant receptors resulted in immunoreactivity of cytosolic structures (Fig. 5, D–F). No specific immunofluorescence was detected in nontransfected unfixed CHO-K1 cells or in transfected cells probed with preimmune serum or antigen-absorbed primary antibody (Fig. 5G). To exclude hsst$_5$r immunostaining of cytosolic structures beneath the membrane as a result of permeabilization of the plasma membrane during incubation with the primary antibody, parallel immunocytochemistry was carried out with antibody to vimentin, an intracellular protein, and showed no surface or cytoplasmic labeling (Fig. 5H). When the cells were permeabilized with 0.2% Triton X-100 before application of vimentin antibody, however, there was intense cytoplasmic staining (Fig. 5I).

Discussion

Using a cassette construct of hsst$_5$R cDNA for the efficient generation of conservative segment exchange and deletion mutants, we mapped the entire exofacial domain of the receptor for potential interaction with SRIF-14, SRIF-28, and SMS ligands. Saturation analysis with ^{125}I-LTT SRIF-28 revealed that mutants of the NH_2-terminal segment of ECL1 and ECL3 were properly expressed and retained high affinity binding. Deletion of the NH_2-terminal domain produced a slight (<2-fold) decrease in binding potency (K_i) for SRIF-14, SRIF-28, and SMS compared with the wild-type construct. hsst$_5$R thus joins other GPCRs, such as TRH and glucagon receptors, whose NH_2-terminal domain does not influence ligand binding (29, 30). Because the NH_2-terminal segment contains two putative *N*-linked glycosylation sites, our results further suggest that glycosylation of hsst$_5$R is not a determinant of high affinity ligand binding. This is in contrast to solubilized rat brain sstRs, which have been reported to lose high affinity agonist binding on deglycosylation (31). Binding of SRIF-14, SRIF-28, and SMS to the CSE mutants of ECL1 and ECL3 was also comparable with that of the wild-type receptor, suggesting that no crucial interaction occurs between the three peptides and residues in ECL1 and ECL3. In contrast, radioligand binding to the two ECL2 mutants was completely abolished. Because the changes introduced are conservative, we cannot rule out the possibility that the altered residues can still interact with the ligand. In this case, the location of the residue would be the determinant of ligand interaction. Using specific antibodies directed against the hsst$_5$R NH_2-terminal segment, the mutant ECL2 receptors were shown by immunocytochemistry to be correctly targeted to the cell surface. Immunocytochemistry using live unfixed cells ensured the integrity of the plasma membrane and established that the hsst$_5$r immunofluorescence was due to membrane and not cytosolic receptors. Thus, failure of the mutant proteins to bind agonist could be explained by a model in which the altered residues represent crucial points of interaction between receptor and ligand. Alternatively, the mutations in ECL2 might have allosterically disrupted the ligand binding pocket. To distinguish

MOL PHARM
MOLECULAR PHARMACOLOGY
aspet

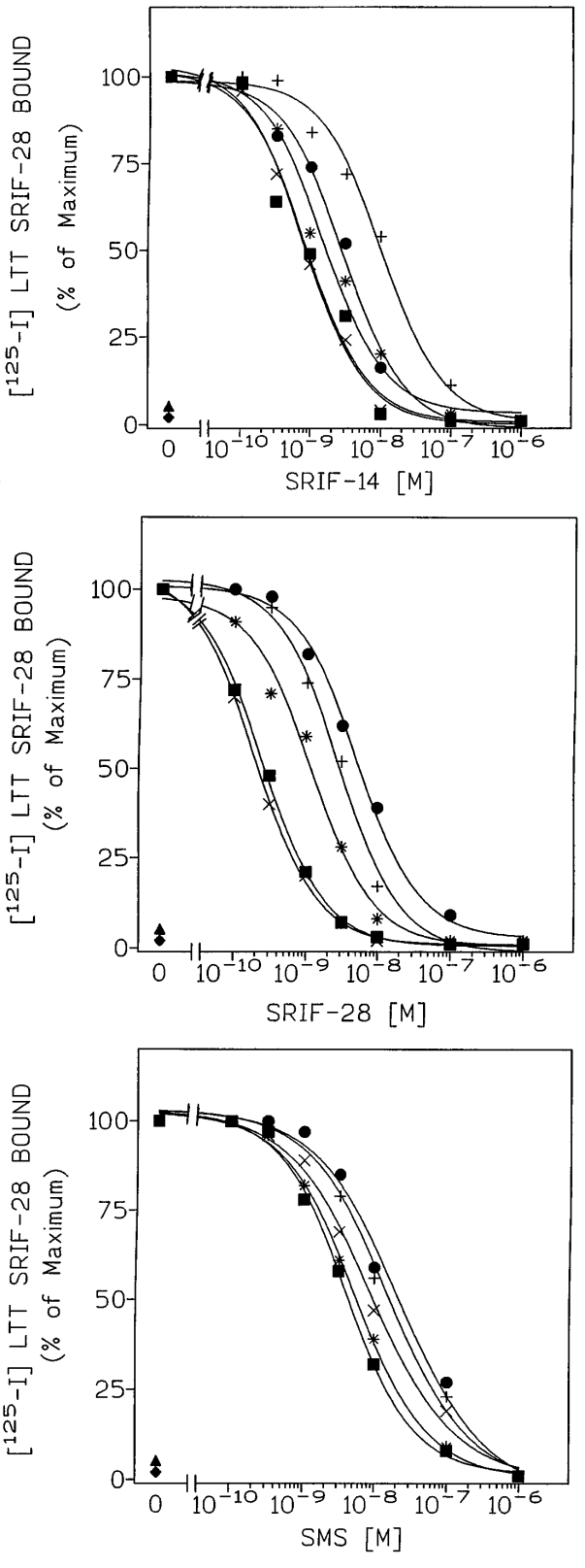

Fig. 4. Competitive binding analyses of hsst$_5$R CSE and amino-terminal deletion mutants. Competitive dose-dependent inhibition of ^{125}I-LTT SRIF-28 binding to hsst$_5$R and hsst$_5$R mutants by SRIF-114, SRIF-28, and SMS. Membranes were prepared from cells stably expressing the wild-type hsst$_5$R cassette construct (■) or Δ5nt mutant (×), mut1 (*), mut2N (▲), mut2C (♦), mut3 (●), and ΔECL3 mutants (+) were incubated with 60 pM ^{125}I-LTT SRIF-28 and the indicated concentrations of SRIF-14 (*top*), SRIF-28 (*middle*), or SMS (*bottom*) under equilibrium conditions (see Experimental Procedures). Error bars were omitted for clarity (n = 3). Total and nonspecific binding of each construct are shown separately in Fig. 3.

between these two possibilities, nonpeptide antagonists, which, in many instances, bind to a region of the receptor separate from that involved in agonist peptide binding, have provided a valuable tool in mutational mapping studies of several GPCR systems (4, 7, 20, 32). For example, CSE mutants of ECL3 of the AT$_1$ receptor display differential loss of binding for the agonist angiotensin II while retaining full binding for the nonpeptide antagonist L-158,809, suggesting that the mutation directly affected the ligand binding cavity without altering overall receptor structure (20). Similar analysis of sstR ECL2 mutants of this study, however, could not be undertaken because of the current lack of sstR nonpeptide antagonists. In view of increasing evidence that different agonists may occupy different binding pockets in the same receptor, another approach is to test the interaction of various agonists with the mutant receptor (9, 17, 20). In the case of sstRs, mutational analyses so far have suggested that the binding pocket for SMS involves residues in TMs exclusively (14). Accordingly, we used ^{125}I-Tyr3 SMS as an alternative ligand to ^{125}I-LTT SRIF-28 to detect binding by the two ECL2 mutants. Neither of the two radioligands bound to these mutants, implying that residues in ECL2 form part of the ligand binding pocket for both ligands or mutations in ECL2 caused a structural change in the receptor with secondary loss of binding. Accumulating evidence now suggests an important role of ECL2 in ligand/receptor interactions with the exterior portions of a number of GPCRs (9). Further studies using point mutations of ECL2 are in progress and should help to clarify which, if any, individual residue in ECL2 is required in ligand binding of sstRs.

Earlier work on the putative residues critical for ligand binding has been reported by two groups who provided a tentative model of the sstR ligand binding crevice (14, 24). Kaupmann *et al.* (14) found that mutating the sst$_1$R residues Q291N in TM-VI and S305F in TM-VII to the corresponding residues of sst$_2$R increased the affinity of sst$_1$R for SMS by 1000-fold (14). Mutation of the conserved aspartic acid residue in TM-III of sst$_1$R, sst$_2$R, and sst$_3$R also abolished ligand binding, but it is not known whether this is due to direct involvement of the residue in the ligand binding pocket or a secondary alteration of the receptor structure (14–16). Using these three identified residues, the known structure of the SMS ligand, and the proposed three-dimensional model of GPCRs (3), Kaupmann *et al.* (14) proposed that the ligand binding pocket of sst$_1$R is lined by residues within TMIII–VII (14). The results of Strnad and Hadcock (16) are also consistent with the notion that short SRIF analogs bind to residues within the TMs (14). Using chimeric mouse sst$_1$R and sst$_2$R, Fitzpatrick and Vandlen (24) reported that substitution of the segment between ECL2 and ECL3 in sst$_1$R with the comparable region in sst$_2$R conferred high affinity binding to MK678, providing evidence that determinants involved in recognizing this ligand reside in the portion of sst$_2$R connecting ECL2 and ECL3. In addition, replacement of ECL3 of sst$_2$R with the corresponding portion of sst$_1$R resulted in a 3000-fold decrease in affinity for MK678 without affecting SRIF-28 binding. These results can be explained by direct

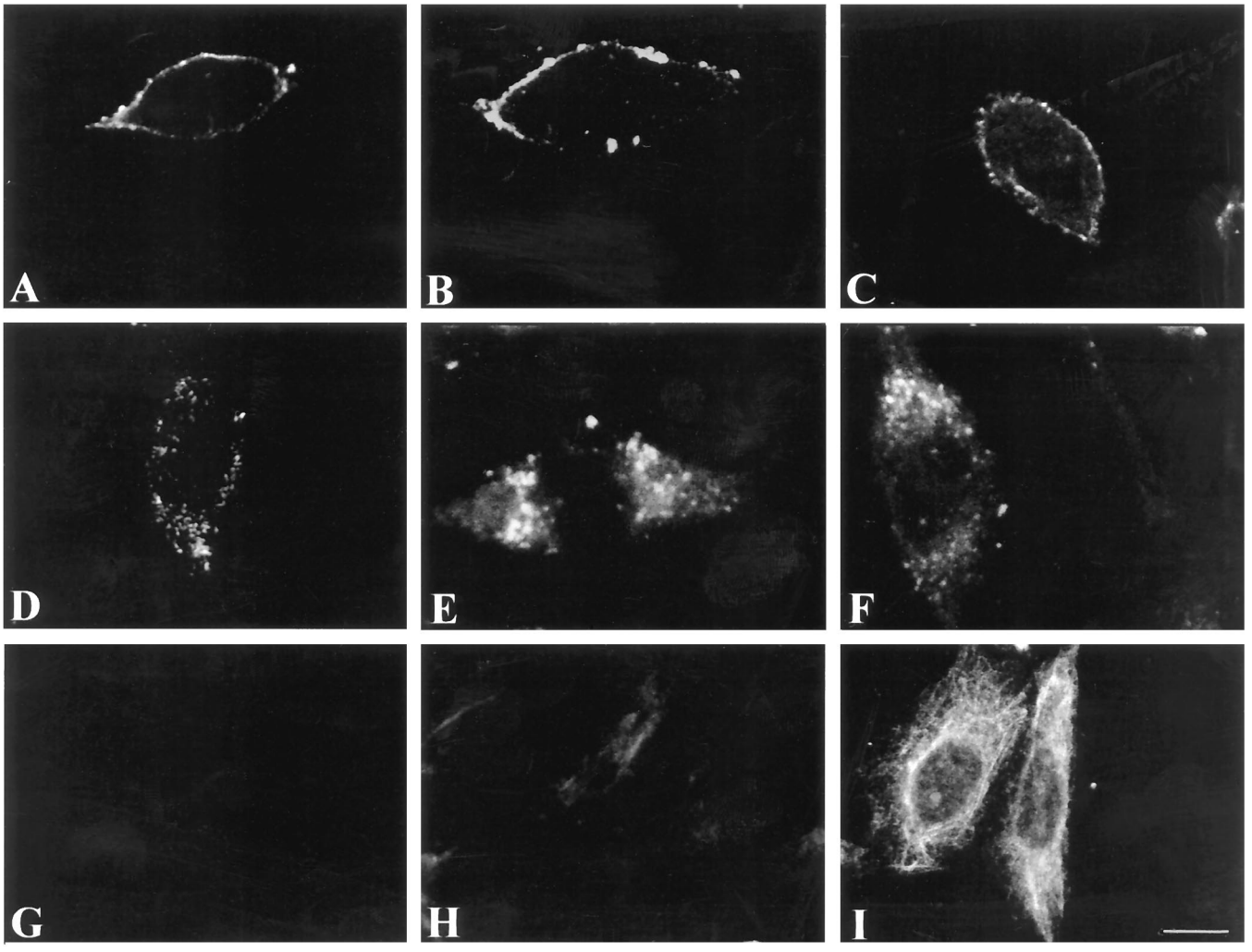

Fig. 5. Immunocytochemical analysis of hsst$_5$R and the ECL2 CSE mutants of hsst$_5$R. Confocal immunohistochemical localization of wild-type and ECL2 mutant hsst$_5$Rs (mut2N, mut2C) in stably transfected CHO-K1 cells. Nonpermeabilized cells (A–C) and Triton X-100-permeabilized cells (D–F) were labeled with rabbit anti-hsst$_5$R primary antibody and rhodamine-conjugated goat anti-rabbit secondary antibody. The integrity of the plasma membrane during the immunohistochemical procedure was monitored in nonpermeabilized and Triton X-100-permeabilized CHO-K1 cells expressing wild-type hsst$_5$R, each immunostained with vimentin antibody under identical conditions as for sst$_5$R localization (H and I). A, Representative unfixed cell expressing wild-type hsst$_5$R displays strong immunofluorescence over the cell surface. mut2N (B) and mut2C (C) in unfixed CHO-K1 cells also display surface immunofluorescence, indicating plasma membrane expression of the mutant receptors. Permeabilization of CHO-K1 cells expressing wild-type (D) mut2N (E), and mut2C (F) results in immunostaining of cytosolic structures. Specificity of sst$_5$R fluorescence was validated using nontransfected unfixed CHO-K1 cells (G) or with preimmune serum and antigen-absorbed antibody (not shown). Specific vimentin immunoreactivity was undetectable in nonpermeabilized CHO-K1 cells expressing wild-type hsst$_5$R (H) but readily detectable in permeabilized cells (I). *Scale bar*, 10 μM.

involvement of the ECL3 of sst$_2$R in MK678 binding or by the relatively short ECL3 of sst$_1$R sterically hindering access of MK678 to the ligand binding pocket. Such a role of ECLs in ligand exclusion has been proposed for other GPCRs (31). In this study, truncation of the ECL3 of hsst$_5$R to mimic the size of this loop in sst$_1$R produced only a modest 3-fold decrease in affinity for SMS. Furthermore, in the Fitzpatrick and Vandlen study (24), the putative ECL3 segment of sst$_1$R grafted onto sst$_2$R consisted not only of ECL3 but also the upper helices of TMVI and TMVII, which contain residues N and FDFV, which are critical for binding. Thus, neither the size of ECL3 nor individual residues seem to be determinants of SRIF binding or of the low affinity of sst$_1$R for the short SRIF analogs. It should be noted that of all the residues identified by mutagenesis as being important in recognizing SMS and MK678, none have been shown to be critical for binding the natural ligands SRIF-14 and SRIF-28 (14, 24). Furthermore, the assumption by Kaupmann *et al.* (14) that sst$_2$R shares a common ligand binding pocket with the other sstRs may not be generally applicable because there are several examples suggesting that closely related GPCRs feature different sets of epitopes for binding of a common ligand (18–20). For instance, some residues of the AT$_1$ receptor that have been shown to be involved in ligand binding are not conserved in the AT$_2$ receptor even though the two receptors bind the same ligand (20). Overall, in combining our results with those obtained by Kaupmann *et al.* (14), the model that emerges suggests a binding pocket for SRIF ligand lined by residues within TMIII–VII with a potential contribution by ECL2. Such a model is consistent with other peptide binding GPCRs, such as neurokinin$_1$, AT$_2$, gonadotropin-releasing hormone, and luteinizing hormone-re-

leasing hormone, that interact with residues in both ECLs and TMs (8, 20, 34).

Acknowledgments

We thank Dr. D. Laird for the vimentin antibody, M. Suresh and O. Dembinska for their assistance, and M. Correia for secretarial help.

References

1. Dohlman, H. G., J. Thorner, M. G. Caron, and R. J. Lefkowitz. Model systems for the study of seven-transmembrane-segment receptors. *Annu. Rev. Biochem.* **60:**653–688 (1991).
2. Schertler, G. F. X., C. Villa, and R. Henderson. Projection structure of rhodopsin. *Nature (Lond.)* **362:**770–772 (1993).
3. Baldwin, J. M. The probable arrangement of the helices in G protein-coupled receptors. *EMBO J.* **12:**1693–1703 (1993).
4. Schwartz, T. W. Locating ligand-binding sites in 7TM receptors by protein engineering. *Curr. Opin. Biotech.* **5:**434–444 (1994).
5. Houslay, M. D. G-protein linked receptors: a family probed by molecular cloning and mutagenesis procedures. *Clin. Endocrinol.* **36:**525–534 (1992).
6. Balwin, J. M. Structure and function of receptors coupled to G proteins. *Curr. Opin. Cell Biol.* **6:**180–190 (1994).
7. Strader, C. D., T. M. Fong, M. P. Graziano, and M. R. Tota. The family of G-protein-coupled receptors. *FASEB J.* **9:**745–754 (1995).
8. Gether, U., T. E. Johansen, R. M. Snider, J. A. Lowe, X. Emonds-Alt, Y. Yokota, S. Nakanishi, and T. W. Schwartz. Binding epitopes for peptide and non-peptide ligands on the NK1 (substance P) receptor. *Regul. Pept.* **46:**49–58 (1993).
9. Schwartz, T. W., and M. M. Rosenkilde. Is there a lock for all agonist keys in 7TM receptors? *Trends Pharmacol. Sci.* **17:**213–216 (1996).
10. Patel, Y. C., M. T. Greenwood, R. Panetta, L. L. Demchyshyn, H. B. Niznik, and C. B. Srikant. The somatostatin receptor family: a mini review. *Life Sci.* **57:**1249–1265 (1995).
11. Panetta, R., M. T. Greenwood, A. Warszynska, L. L. Demchyshyn, R. Day, H. B. Niznik, C. B. Srikant, and Y. C. Patel. Molecular cloning, functional characterization, and chromosomal localization of a human somatostatin receptor (somatostatin receptor type 5) with preferential affinity for somatostatin-28. *Mol. Pharmacol.* **45:**417–427 (1994).
12. Patel, Y. C., and C. B. Srikant. Subtype selectivity of peptide analogs for all five cloned human somatostatin receptors (hsstr1–5). *Endocrinology* **135:**2814–2817 (1994).
13. Bruns, C., G. Weckbecker, F. Raulf, K. Kaupmann, P. Schoefter, D. Hoyer, and H. Lübbert. Molecular pharmacology of somatostatin-receptor subtypes. *Ann. N. Y. Acad. Sci.* **733:**138–146 (1994).
14. Kaupmann, K., C. Bruns, F. Raulf, H. P. Weber, H. Mattes, and H. Lübbert. Two amino acids, located in transmembrane domains VI and VII, determine the selectivity of the peptide agonist SMS 201–995 for the SSTR2 somatostatin receptor. *EMBO J.* **14:**727–735 (1995).
15. Nehring, R. B., W. Meyerhof, and D. Richter. Aspartic acid residue 124 in the third transmembrane domain of the somatostatin receptor subtype 3 is essential for somatostatin-14 binding. *DNA Cell Biol.* **14:**939–944 (1995).
16. Strnad, J., and J. R. Hadcock. Identification of a critical aspartate residue in transmembrane domain three necessary for the binding of somatostatin to the somatostatin receptor SSTR2. *Biochem. Biophys. Res. Commun.* **216:**913–921 (1995).
17. Pradier, L., J. Menager, J. Le Guern, M.-D. Bockj, E. Heuillet, V. Fardin, C. Garret, A. Doble, and J.-F. Mayaux. Septide: an agonist for the NK1 receptor acting at a site distinct from substance P. *Mol. Pharmacol.* **45:** 287–293 (1994).
18. Gingrich, J. A., and M. G. Caron. Recent advances in the molecular biology of dopamine receptors. *Annu. Rev. Neurosci.* **16:**299–321 (1993).
19. Humphrey, P. P. A., P. Hartig, and D. Hoyer. A proposed new nomenclature for 5-HT receptors. *Trends Pharmacol. Sci.* **14:**233–236 (1993).
20. Hjorth, S. A., H. T. Schambye, W. J. Greenlee, and T. W. Schwartz. Identification of peptide binding residues in the extracellular domains of the AT1 receptor. *J. Biol. Chem.* **269:**30953–30959 (1994).
21. Kozak, M. An analysis of 5′-noncoding sequences from 699 vertebrate messenger RNAs. *Nucleic Acids Res.* **15:**8125–8148 (1987).
22. Johansen, T. E., M. S. Scholler, S. Tolstoy, and T. W. Schwartz. Biosynthesis of peptide precursors and protease inhibitors using new constitutive and inducible eukaryotic expression vectors. *FEBS Lett.* **267:**289–294 (1990).
23. Probst, W. C., L. A. Snyder, D. I. Schuster, J. Brosius, and S. C. Sealfon. Sequence alignment of the G-protein coupled receptor superfamily. *DNA Cell Biol.* **11:**1–20 (1992).
24. Fitzpatrick, V. D., and R. L. Vandlen. 6Agonist selectivity determinants in somatostatin receptor subtypes I and II. *J. Biol. Chem.* **269:**24621–24626 (1994).
25. Horton, R. M., H. D. Hunt, S. N. Ho, J. K. Pullen, and L. R. Pease. Engineering hybrid genes without the use of restriction enzymes: gene splicing by overlap extension. *Gene* **77:**61–68 (1989).
26. Ho, S. N., H. D. Hunt, R. M. Horton, J. K. Pullen, and L. R. Pease. Site-directed mutagenesis by overlap extension using the polymerase chain reaction. *Gene* **77:**51–59 (1989).
27. Srikant, C. B., and Y. C. Patel. Somatostatin receptors: identification and characterization in rat brain membranes. *Proc. Natl. Acad. Sci. USA* **78:**3930–3934 (1981).
28. Hukovic, N., R. Panetta, U. Kumar, and Y. C. Patel. Agonist-dependent regulation of cloned human somatostatin receptor types 1–5 (hSSTR1–5): subtype selective internalization or upregulation. *Endocrinology* **137:** 4046–4049 (1996).
29. Han, B., and A. H. Tashjian, Jr. Importance of extracellular domains for ligand binding in the thyrotropin-releasing hormone receptor. *Mol. Endocrinol.* **9:**1708–1719 (1995).
30. Unson, C. G., A. M. Cypess, H. N. Kim, P. K. Goldsmith, C. J. L. Carruthers, R. B. Merrifield, and T. P. Sakmar. Characterization of deletion and truncation mutants of the rat glucagon receptor: seven transmembrane segments are necessary for receptor transport to the plasma membrane and glucagon binding. *J. Biol. Chem.* **270:**27720–27727 (1995).
31. Rens-Domiano, S., and T. Reisine. Structural analysis and functional role of the carbohydrate component of somatostatin receptors. *J. Biol. Chem.* **266:**20094–20102 (1991).
32. Rosenkilde, M. M., M. Cahir, U. Gether, S. A. Hjorth, and T. W. Schwartz. Mutations along transmembrane segment II of the NK-1 receptor affect substance P competition with non-peptide antagonists but not substance P binding. *J. Biol. Chem.* **269:**28160–28164 (1994).
33. Metzger, T. G., and D. M. Ferguson. On the role of extracellular loops of opioid receptors in conferring ligand selectivity. *FEBS Lett.* **375:**1–4 (1995).
34. Flanagan, C. A., I. I. Becker, J. S. Davidson, I. K. Wakefield, W. Zhou, S. C. Sealfon, and R. P. Millar. Glutamate 301 of the mouse gonadotropin-releasing hormone receptor confers specificity for arginine 8 of mammalian gonadotropin-releasing hormone. *J. Biol. Chem.* **269:**22636–22641 (1994).

Send reprint requests to: Dr. Y. C. Patel, Royal Victoria Hospital, 687 Pine Avenue West, Montreal, Quebec H3A 1A1, Canada. E-mail: patel@rvhmed.lan.mcgill.ca